Audiological Medicine, 2010; Early Online, 1–10

informa
healthcare

ORIGINAL ARTICLE

The inner ear phenotype of Volchok (Vlk): An ENU-induced mouse model for CHARGE syndrome

DANIELLE R. LENZ[1], AMIEL A. DROR[1], GUY WEKSELMAN[1], HELMUT FUCHS[2], MARTIN HRABÉ DE ANGELIS[2] & KAREN B. AVRAHAM[1]

[1]*Department of Human Molecular Genetics and Biochemistry, Sackler Faculty of Medicine, Tel Aviv University, Tel Aviv, Israel,* [2]*Institute of Experimental Genetics, Helmholtz Zentrum München Neuherberg, Germany*

Abstract

Objective: The Volchok (Vlk) mouse originated as a part of a large-scale ENU program on a C3HeB/FeJ background. The mice present a dominant pattern of inheritance reflected mainly by circling activity, which led us to search for the causative mutation underlying the vestibular phenotype. *Study design:* Linkage analysis and subsequent sequencing were used to narrow down the genomic region and uncover the mutation, respectively. Behavioral analysis and examination of the inner ear phenotype was performed using the modified SHIRPA protocol, auditory brainstem response (ABR), immunofluorescence, light microscopy, scanning electron microscopy (SEM), paint-fill and neurofilament staining techniques. *Results:* A nonsense mutation was discovered in the Chd7 gene responsible for CHARGE syndrome in humans, which leads to a decrease in Chd7 expression in the nuclei of the vestibular and cochlear cells and structural abnormalities in the inner ear. A mild hearing loss was found in the mutant mice. The malformations detected include a truncated lateral semicircular canal and smaller lateral crista, a decrease in size or absence of the round window in the cochlea and lack of innervations to the posterior crista. *Conclusion:* Vlk joins a series of previously characterized mice bearing a Chd7 mutation, linking abnormalities found both in ENU-induced mutants and a knock-out mouse model. Combining the information from multiple Chd7 alleles provides a more comprehensive understanding of the mechanisms underlying this human disease.

Key words: *CHD7, vestibule, cochlea, hearing loss*

Introduction

The mammalian inner ear comprises the cochlear and vestibular labyrinths that enable the perception of sound and balance, respectively (1,2). The vestibular system transduces changes in acceleration and position of the body to nerve stimuli, adjusting the body in relation to the environment. Mismatches such as dizziness, nausea and even vertigo may occur when going on a roller-coaster or a boat trip or as a result of various abnormalities in the vestibular end-organs. Mutations in several genes have been reported to be associated with vestibular pathologies, encouraging geneticists to continue the search for more genes and mechanisms underlying different malformations both in humans and in different animal models (3,4).

In the vestibular system, the two gravity receptor organs, utricle and saccule, control the sense of linear acceleration and gravity, whereas the three semicircular canals and their cristae are responsible for the sense of angular acceleration (1,2). These two types of movements compose our sense of balance. Hearing and balance are both dependent on the movement of the endolymphatic fluid in the inner ear, causing a change in mechanosensory cells, referred to as hair cells, which cover the area of the organ of Corti in the cochlea and the three cristae, utricle and saccule in the vestibule. Dependent on the orientation of the stereocilia, the cells experience either depolarization or hyperpolarization of the membrane. Depolarization results in excitation of the axon connected to the hair cell, whereas hyperpolarization inhibits the axon's

Correspondence: K. B. Avraham, Department of Human Molecular Genetics and Biochemistry, Sackler Faculty of Medicine, Tel Aviv University, Tel Aviv 69978, Israel. Tel: +972 3 6407030. Fax: +972 3 6409360. E-mail: Karena@post.tau.ac.il

ISSN 1651-386X print/ISSN 1651-3835 online
DOI: 10.3109/1651386X.2010.490039

activity. These axons are part of the vestibulo-cochlear nerve, thus the changes in their firing rates are transduced to the cochlear and vestibular nuclei where interpretation of sound and the position of the head are being performed, respectively (2). In the cristae, a gelatinous component, the cupula, covers the hair cells and monitors their movement. When the head is turned in a certain direction the endolymphatic fluid accelerates within the canals in the opposite direction at first, and only later coincides with the head's angular motion. Deceleration or complete stop results in a similar process in the opposite direction. It should be noted that the vestibular organs are located in opposite directions on both sides of the head, thus in any given movement several hair cells are excited while others are inhibited, resulting in a vast range of possible positions the nervous system can interpret (2).

Mice are the most relevant organism to study biological processes and pathogenesis of human disease due to genetic and functional similarities between humans and mice. In this regard, phenotype-driven mutagenesis screens to generate N-ethyl-N-nitrosourea (ENU) mouse models that display hearing impairment and/or vestibular dysfunction have been an extremely important tool for the isolation and identification of novel genes (5). ENU-generated mutant mice present an excellent animal model, reflecting the heterogeneity of these phenotypes. The genotype and phenotype of these mice are analysed in order to uncover novel genes, shedding light on the mechanisms causing inner ear abnormalities.

Cochlear and vestibular deficits can appear both in non-syndromic form and as a part of various syndromes. When resulting from a structural malformation, they are usually innate, while dysfunction caused by loss of hair cells or otoconia displacement can have a late onset and be subjected to environmental aspects, such as head trauma, various drugs, viral infection, prolonged exposure to changes in gravity, etc. (6,7). Ménière's disease is an example of the latter, when presumably calcium carbonate crystals from the otoconia create tiny hydrops that in turn change the flow of the endolymphatic fluid, resulting in vertigo episodes. The above phenomena can be both innate or a consequence of perfuse alcohol consumption, cigarette smoking, head trauma, etc. (8). CHARGE syndrome (OMIM #214800), on the other hand, results from a range of mutations (usually de novo) in the Chromodomain helicase DNA-binding protein 7 (*CHD7*) and is characterized by Coloboma of the eye, Heart defects, Atresia of the choanae, Retarded growth, Genital anomalies and Ear deformations (CHARGE). The variety of abnormalities is a result of the ubiquitous *CHD7* expression and its function as a regulator upstream to various transcription factors during early developmental stages (9). Deletions or single nucleotide substitutions, which result in missense, nonsense or splice-site mutations, cause depletion in the amount of functional protein and consequent manifestations in a variety of organs due to haploinsufficiency (10). In the inner ear, these mutations result in several structural abnormalities, in particular in the vestibule but also in the cochlea. It was previously shown that CHARGE patients' vestibular abnormalities include hypoplasia or complete absence of semicircular canals (11,12). In the mouse inner ear, *Chd7* mutations have been reported to result mainly in truncation of the lateral semicircular canal, but also in anomalies of the posterior semicircular canal and adjacent crista. In addition, ossicles malformations have also been described (10,13). Today, there are no effective long-term treatments for these pathologies, apart from repeated manoeuvres, aimed at providing partial relief and an attempt to use cochlea implantation surgery and develop similar vestibular prostheses (6). Therefore, it is essential to research all aspects, in the hope of a better understanding and development of more effective treatments and cures.

The Volchok mouse (*Vlk*) described in this report originated in a large-scale ENU programme, as part of an attempt to create mice bearing mutations that influence the normal function of the inner ear. *Vlk* mice are identified because of a circling behaviour, representing a structural abnormality in the vestibular system, but also hearing loss. The molecular phenotype observed resembles the already described phenotype of multiple *Chd7* mutants (10,13). Our new finding of a reduction of *Chd7* expression due to the null mutation confirms the *Vlk* mouse as a model for human CHARGE syndrome.

Materials and methods

Mice

The founder of the Volchok strain was generated in a large-scale N-ethyl-N-nitrosourea (ENU) mutagenesis programme (5). All procedures involving animals met the guidelines described in the National Institutes of Health Guide for the Care and Use of Laboratory Animals, and have been approved by the Animal Care and Use Committee of Tel Aviv University, number M-07-061. The gene name and symbol, Volchok *(Vlk)*, was approved by the International Committee on Standardized Genetic Nomenclature for Mice (www.informatics.jax.org).

Genetic mapping and DNA sequencing

In the process of mapping the mutation underlying the phenotype, mutant males were outcrossed to

C57BL/6J females in order to generate hybrid mice, which were subsequently back-crossed to C3HeB/FeJ females. Twenty-one mice that were generated by this cross and presented a clear circling phenotype were used for mapping. Genomic DNA was extracted and analysed using 59 simple sequence-length polymorphism (SSLP) markers that span the entire mouse genome and differ between C3HeB/FeJ and C57BL/6J strains by at least 8 bp (based on the MIT Genome Center genetic map data at http://mouse.ski.mskcc.org/marker/MIT/index.php). Sequencing of the *Chd7* gene was performed (primers available by request from authors) and the mutation was detected in exon 19 with the forward primer 5'-ggctccactggctgttttt-3' and the reverse primer 5'-gaaaggccaatgttctgcat-3'.

Behavioural analysis

The general behaviour and vestibular function of nine mutant mice were compared to the wild-type behaviour of 17 littermates using several tests, performed on an empty large platform that was thoroughly cleaned between each mouse. These tests reflect ability of the mice to sense gravity and perceive their sense of balance. Mice were given 2 min to adjust, followed by 2–3 min in which their general behaviour was tested using the modified SHIRPA protocol that included the following criteria (14).

Reaching response. Mice were held by their tail and lifted above a known platform. Scores were given according to the ability of each mouse to stretch in the direction of the platform: 1.0 for complete stretching of its forelimbs toward the platform, 0.0 for complete curling toward its belly.

Circling and head bobbing behaviour. During 2–3 min, mice were observed on a platform and the amount of time spent circling and head bobbing was measured. Mice presenting an excessive circling or bobbing behaviour were given the score 1.0; no such behaviour was scored 0.0; and slight behaviour was scored 0.5.

Swim test. An empty box (45 cm wide, 30 cm long and 20 cm deep) was filled with water at 25°C. Mice were dropped in and the general pattern of behaviour in water was analysed for 1–2 min. The mice were taken out and given sufficient time to dry out, as this was the last test conducted at all trials. During the test two qualities were examined: 1) vigour swim – the movement of the mouse's limbs; 2) body above water – which organs the mouse can maintain above water. Scores for vigour swim were given accordingly: 0.0 if the mouse froze and did not move at all; 0.5 if the mouse occasionally moved its hind limbs; 1.0 if the mouse occasionally moved its forelimbs; 1.5 if the mouse floated but did not swim; 2.0 if the mouse occasionally stopped swimming and floated; 2.5 if the mouse swam using only its hind limbs; and 3.0 if the mouse swam with all forelimbs. Scores for body above water were given accordingly: 0.0 if the whole body submerged in the water; 0.5 if the mouse could not keep its head above water; 1.0 if the mouse kept only its nose above water; 1.5 if the mouse kept its eyes at water level; 2.0 if the mouse could not keep its ears above water; 2.5 if the mouse's head was above water; and 3.0 if the mouse's head and back were above water.

Auditory brainstem response (ABR)

The founders of the *Vlk* colony were originally described as hearing according to their Preyer reflex. We repeated the examination using a click box apparatus, which produces a sharp sound at a constant frequency and amplitude of 20 kHz and 96dB, respectively. The sound stimulus causes normal mice to exhibit a Preyer reflex, a distinctive back movement of the pinna, demonstrating a normal response of hearing at this range. However, since this test does not reflect mild hearing loss across the entire spectrum we also performed ABR (Intelligent Hearing Systems). At P60, nine mutant and 17 wild-type littermates were examined. Mice were anaesthetized using an injection of avertin (dosage dependent on mouse weight), and placed on a preheated platform. Three electrodes were subdermally connected at the leg, forehead and throat, and a sound conductive tube was placed in the right ear. Three frequencies were examined for evaluation of the hearing ability throughout the spectrum: 8 kHz, 16 kHz and 32 kHz. At each frequency, sound pressure levels (SPL) ranging between 20 and 100dB were analysed in order to assess the threshold. Thresholds were determined according to the last SPL demonstrating a coherent wave containing four peaks, at exactly the same location in every repeat of the test.

Immunofluorescence staining

Inner ears were dissected out and fixed using 4% paraformaldehyde (PFA) overnight at 4°C. Ears from adult mice at P90 were fixed and decalcified for 2 h using Bouin's solution (Sigma). For further analysis using paraffin sections, ears were processed using a paraffin embedding robot (JUNG Histoembedder, Leica), positioned in paraffin blocks and sectioned using a microtome (JUNG RM2055, Leica). Paraffin was removed using xylene followed by rehydration and incubation with previously boiled antigen unmasking solution (H-3300, Vector). Slides were then incubated with a blocking solution containing 0.2% gelatin in 0.2% PBST (PBS with 0.2% Tween 20) and further stained with primary and secondary

antibodies as described for whole-mounted tissue samples.

For further analysis of whole-mount tissue samples, ears were fine-dissected and the sensory epithelia were exposed. Permeabilization and blocking were conducted using 0.5% Triton in PBS and PBS containing 1% bovine serum albumin (BSA) and 10% normal goat serum, respectively. Samples were stained overnight at 4°C with the primary antibodies: rabbit anti-Chd7 (Abcam), mouse anti-neurofilament (Sigma), goat anti-myosin VI (Santa Cruz) and rabbit anti-myosin VI (Proteus). Samples were then incubated with compatible secondary antibodies (Alexa fluor 488 and 594, Molecular Probes) and Alexa-568 conjugated phalloidin (Molecular Probes) and mounted. All pictures were taken using the LSM 510 confocal microscope (Zeiss).

Scanning electron microscope (SEM)

Inner ears were dissected out in 0.1 *M* sodium phosphate buffer and fixed in 2.5% gluteraldehyde diluted in 0.1 *M* sodium phosphate overnight at 4°C. Fine dissection was conducted in order to expose the sensory epithelia. Preparation of the samples was performed using the osmium tetroxide-thiocarbohydrazide (OTOTO) protocol (15). Samples were transferred to critical point dry and gold coverage procedures at the Faculty of Life Sciences Electron Microscopy Unit and scanned using the JSM 840A scanning electron microscope (Jeol).

Paint fill

The heads of P0 mice were bisected and fixed in Bodian's fixative overnight at 4°C. Half-heads were dehydrated using increasing percentages of ethanol, two rinses per percentage, each for 2 h. Half-heads were then placed in methyl salicylate overnight and kept in a chemical hood. Paint filling was subsequently conducted as described by Bissonnette and Fekete (16) using a glass capillary pipette filled with paint, which was injected into the common crus or the area between the utricle and posterior crista.

Results

A nonsense mutation in Chd7 is responsible for the Vlk/+ phenotype

A genome-wide scan was conducted including three markers for chromosome 4 (D4Mit235, D4Mit149 and D4Mit193) and revealed linkage to the subcentromeric marker D4Mit235. Due to phenotypic similarities with previously described *Chd7* mutants (10,17), we predicted that the mutation occurred in the *Chd7* gene and subsequently sequenced the entire gene. Sequence analysis of exon 19 revealed a T-to-A transversion at position 4705 (c.T4705A) in the *Vlk* mutants, forming a nonsense mutation (Figure 1A). The mutation is predicted to cause a codon change of TAT to TAA resulting in a substitution of the amino acid tyrosine at position 1459 to a stop codon (p.Y1459X). The protein product of the gene containing the stop codon is truncated after the helicase C-terminal domain. Despite including all predicted functional domains (according to UniProtKB database, www.uniprot.org) (Figure 1B), phenotypic similarities between *Vlk* mutants and previously reported *Chd7* mouse mutants with a null allele suggest that *Chd7* in *Vlk* is non-functional as well. The remaining wild-type allele presumably does not produce enough protein, resulting in the *Vlk* dominant mutation due to haploinsufficiency. *Chd7* mutations have been described as embryonic lethal when homozygous (10). Since we were unable to recover *Vlk* homozygous offspring, we predict that homozygousity is lethal in this case as well.

Reduction in Chd7 expression in Vlk/+ inner ears

The nonsense mutation in the *Chd7* gene results in a null allele in *Vlk* mice, as described above. Immunofluorescent staining of both the cochlear and vestibular sensory epithelia at P0 reveals an obvious reduction in *Chd7* expression in mutant mice (Figure 1C). Previous reports portrayed *Chd7* expression during embryonic development using in situ hybridization (10) and here we present wild-type and mutant expression at P0 by immunohistochemistry. Similarly to embryonic *Chd7*, the expression at P0 can be detected in the nuclei of hair cells and supporting cells in the sensory epithelia, and also in various surrounding cells such as the spiral ganglia (data not shown). In contrast, no *Chd7* expression can be detected in three-month-old mice, presumably due to reduced expression after complete maturation of the inner ear (data not shown).

Vlk/+ behavioural phenotype coincides with the vestibular structural malformations

Vlk/+ mice present a circling behaviour, head bobbing and an abnormal reaching response that become more distinguishable as the mice mature, but can be identified at weaning. At P60 the mice were examined using a set of protocols based on the EMPReSS database (14), and an additional inability to swim was added as one of the distinguishable behavioural phenotypes of this line (Figure 2A).

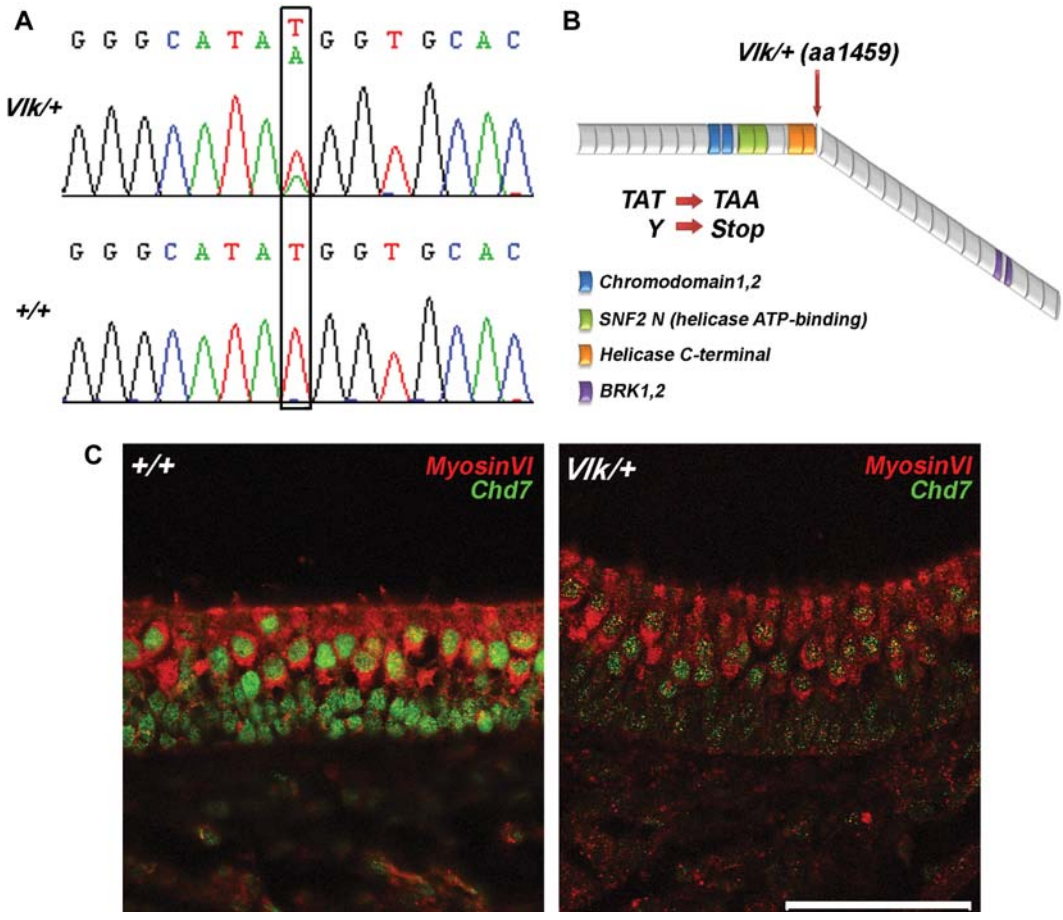

Figure 1. A nonsense mutation in *Chd7* results in a null copy of the gene. ENU random mutagenesis induced a point mutation, resulting in a c.T4705A transversion. (A) Chromatogram analysis of a *Vlk* mutant demonstrates the heterozygous nature of the mutation, presenting one allele with the original T nucleotide and one allele with A. (B) A scheme of the mouse Chd7 protein. Similar to other CHD proteins, Chd7 contains three main functional domains crucial for its role as a transcription regulator involved in chromatin remodelling: a chromodomain (x2), a helicase ATP-binding domain (also referred to as SNF2 N domain) and a helicase C-terminal domain. In addition, Chd7 includes 2 BRK domains, probably responsible for DNA binding. The nonsense mutation Y1459X at exon 19 creates a stop codon, resulting in an affectively null allele. (C) Immunofluorescent staining of paraffin sections of the utricular macula at P0 with Chd7 (green) and the hair cell marker myosin VI (red) demonstrates the decreased *Chd7* expression in the nuclei of the vestibular cells compared to the wild-type expression level.

All *Vlk*/+ mice examined circle and bear abnormalities in the lateral canal and crista, similarly to all previously reported *Chd7* mutants (10,13,18) (Figure 3A,B). The extent of canal truncation and crista reduction vary between different mice and at times even between two ears of the same mouse. Several of the mutant mice present posterior canal and crista anomalies as well. It should be noted that no hair cell abnormalities were detected (Figure 3C).

Vlk/+ mice present higher ABR thresholds with no obvious cochlear abnormality

A Preyer reflex, indicative of hearing, did not reveal any difference between wild-type and mutant littermates. However, the click box apparatus used for this inspection produces a sharp sound at one frequency of 20 kHz, and therefore does not fully represent the auditory spectrum. In contrast, during an ABR experiment three different frequencies are measured (8, 16 and 32 kHz), each by decreasing amplitudes ranging from 100dB to 20dB. A reduction in ABR thresholds was detected in *Vlk* mutant mice (Figure 2B,C). While the most significant difference appeared at 8 kHz, a more subtle but still statistically significant shift was shown at 16 kHz and 32 kHz. In the cochlea, a decrease in size or absence of the round window was detected, observed using light microscopy in four mutant mice (Figure 4A). Immunofluorescent staining and SEM of hair cells and supporting cells both at P0 and adult mice did not reveal any abnormalities (Figure 4B,C).

Lack of innervations to the posterior crista in Vlk/+

In mice that are heterozygous for a *Chd7*-deficient, gene-trapped allele, various vestibular abnormalities

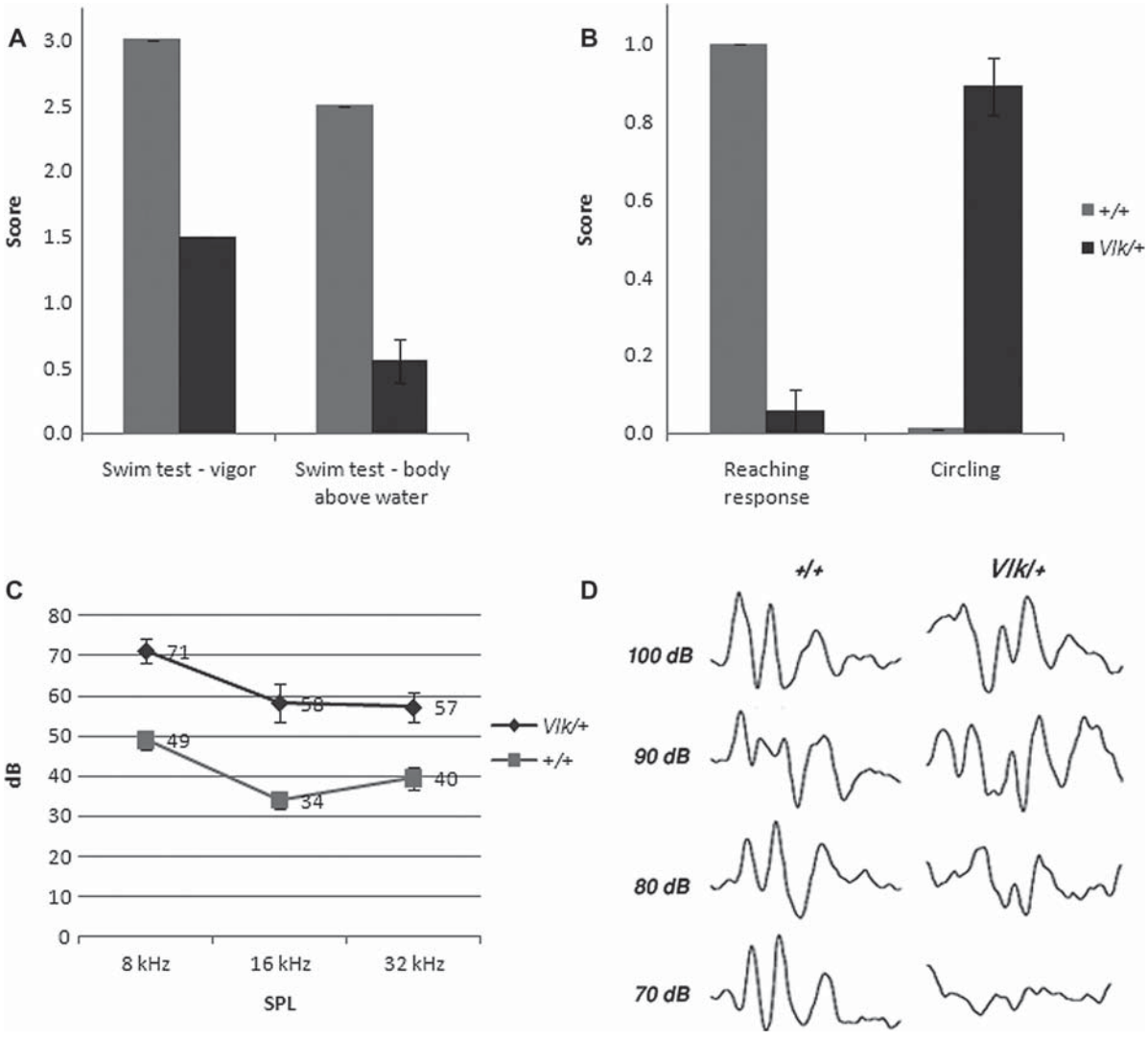

Figure 2. Significant differences in behavioural tests present vestibular and cochlear abnormalities. Swimming (A), circling and reaching response (B) tests, representing vestibular abnormalities in the mutant *Vlk* mice. (C) ABR results show a significant increase in hearing thresholds of *Vlk*/+ mice at all three frequencies, implying a mild hearing loss. The difference is the most significant at the lowest frequency (8 kHz; p-value $= 2.8 \times 10^{-5}$), reflecting damage in the apex of the cochlea. Both ABR and vestibular test results are statistically significant according to a Student's t-test (p-value $<<0.05$) and all bars represent standard error of mean. (D) An example of ABR results from wild-type and mutant *Vlk* littermates at P60. The peaks represent the transition of signals through the nerve fibres from the cochlea to the auditory cortex. In the mutant, the peaks' amplitude decreases rapidly while in the wild type, the peaks continue to appear strong and coherent.

were described, including lack of innervation to the posterior crista (13). Immunofluorescent staining of paraffin embedded sections and whole-mount tissue at P90 and two-year-old mice revealed that *Vlk*/+ mice also present the same abnormality (Figure 5).

Discussion

Different types of abnormalities can cause vestibular pathologies in CHARGE syndrome, Alagille syndrome, Ménière's disease, superior canal dehiscence syndrome and others, resulting in dizziness, vertigo, nausea, tinnitus, positional nystagmus and even inability to stand straight and move the head (2,6). Some studies have also linked vestibular dysfunction with increased anxiety and spatial memory loss (19,20). Various genes have been linked to the above mentioned pathologies, emphasizing the importance of research conducted in the field in the hope of finding various solutions. As part of the above mentioned effort, ENU mutagenesis programmes created mouse mutants that serve as models for various human diseases such as hearing loss and vestibular dysfunction (4,5). One of these mouse models is Volchok, which we present in this report. The *Vlk* mutation is dominant with a predicted null allele due to a nonsense mutation, and the mice present circling and head bobbing behaviour in addition to mild hearing loss.

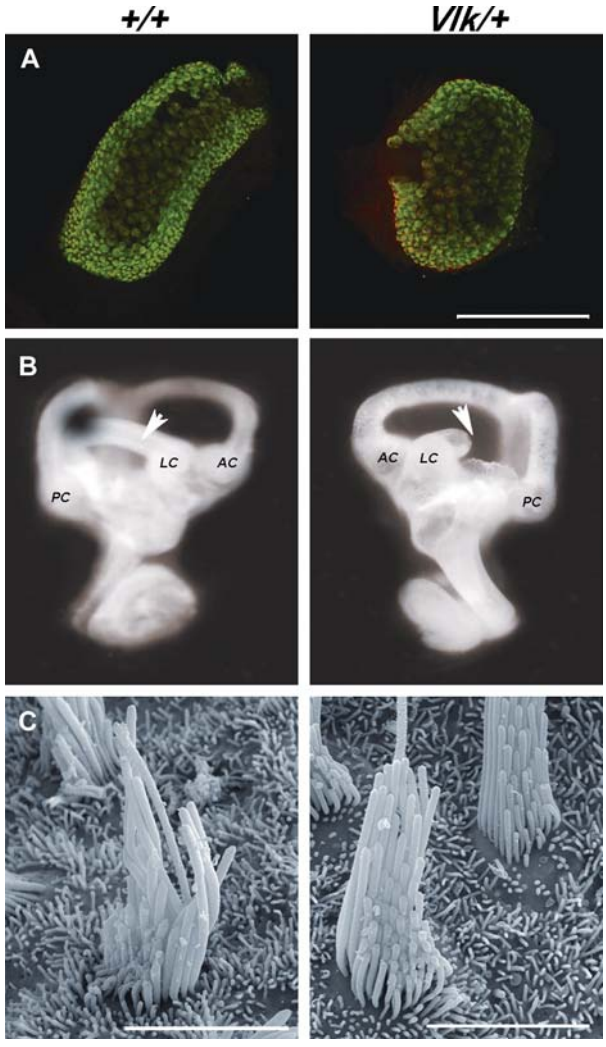

Figure 3. Vestibular structural malformations appear in *Vlk*/+ mice. *Vlk* mutant mice present a behaviour indicative of vestibular anomalies. (A) The lateral crista is smaller, as can be seen by immunofluorescent staining at P0 with the hair cell marker myosin VI (green) and phalloidin (red), which stains actin. (B) The lateral semicircular canal is truncated (arrowhead), as demonstrated using paint fill analysis. (C) Hair cells in the vestibular system appear normal by SEM. PC: posterior crista; AC: anterior crista; LC: lateral crista. Scale bars: 200 μm (A), 5 μm (C).

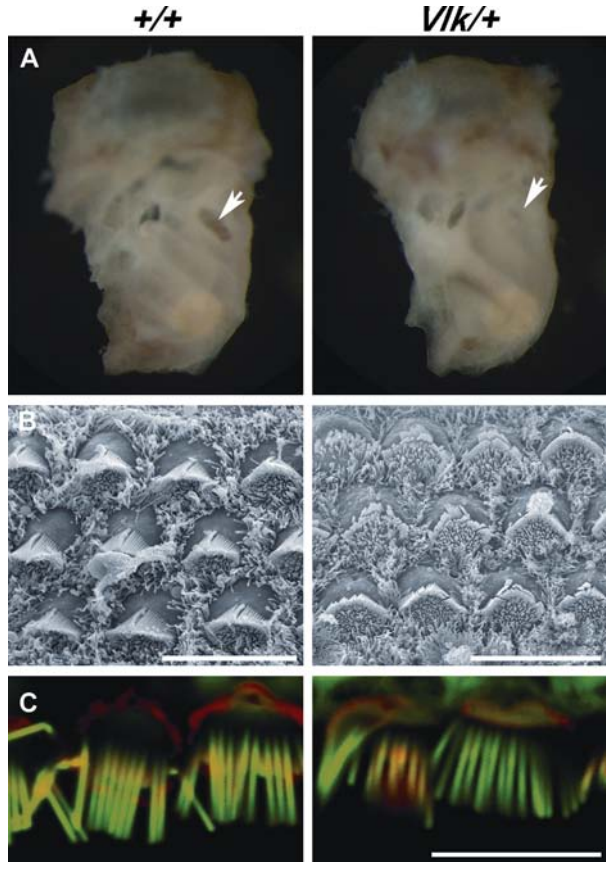

Figure 4. Cochlear structural manifestations in *Vlk*/+ mice. (A) In the cochlea, the structural abnormality detected is a decrease in size or absence of the round window (arrowhead), here seen using light microscopy of a two-year-old mutant mouse and wild-type control. Both inner and outer hair cells of the cochlear sensory epithelium appear normal: (B) SEM images of outer hair cells from P0 mutant and wild-type littermates; (C) immunofluorescent staining of inner hair cells from two-year-old mutant mouse and control, stained with myosin VI (green) and phalloidin (red). Scale bars: 10 μm.

Previous studies dealing with mice presenting compound behavioural abnormalities as seen in the *Vlk* mutants have demonstrated a correlation between circling activity and the malformations of the lateral semicircular canal and crista (13). Since the lateral semicircular canal and adjacent crista are responsible for the sense of right and left movement, referred to as 'yaw' (similar to the movement of saying "no"), the circling action is a plausible reaction of the brain to its inability to sense this motion. Similarly, the head bobbing phenotype can be correlated to the lack of innervations to the posterior crista, as the posterior semicircular canal and crista account for the 'pitch' movement (similar to the movement of saying "yes"). These phenotypic variations that appear as incomplete penetrance are the cause of the behavioural differences between mutant littermates, and are probably the reason why some of the mutants can be identified at P21, while others, carrying a more subtle malformation, present an obvious mutant behaviour only at a later age.

The hearing loss phenotype observed in *Vlk* mutants could not be accounted for. The ability to hear a variety of sounds is partially based on the principle of tonotopy, or the organization of perception in a frequency dependent manner (21). As part of this principle, the cochlear apex is responsible for receiving low tone signals and the base of the cochlea for high tone signals. *Vlk* mice present a more significant reduction in thresholds at lower frequencies, which led us to search for an abnormality in the apex. In contrast to the vestibular dysfunction, no apparent correlated abnormality was identified in the apical or

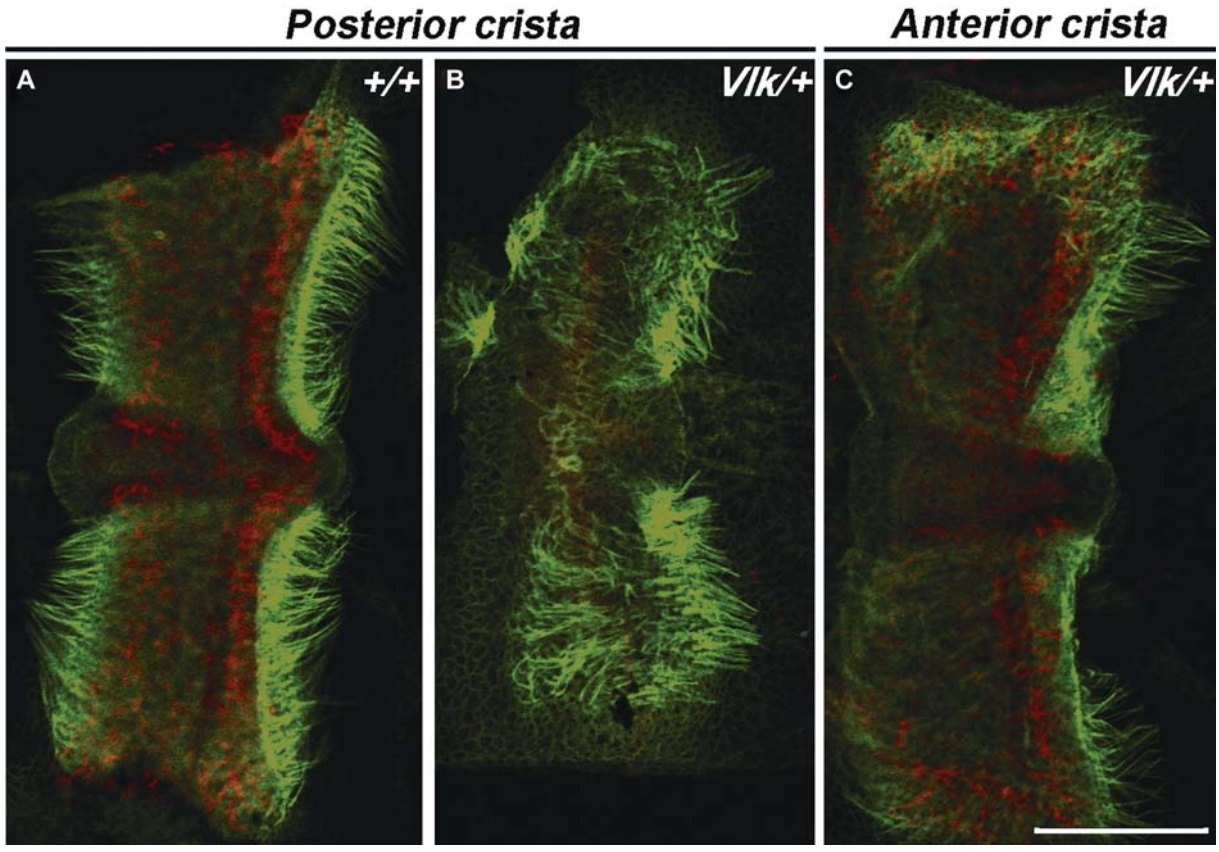

Figure 5. Lack of innervations to the posterior crista in *Vlk*/+ mice. Whole mount immunofluorescent staining of wild-type and mutant cristae of two-year-old mice. Normal innervations are seen in the wild-type posterior crista (A) and in the mutant anterior crista (B) but not in the mutant posterior crista (C). Neurofilament was used as a nerve fibre marker (red) and phalloidin stains the cell borders and stereocilia (green). Scale bar: 100 μm.

basal sensory epithelia or in the adjacent tissues of the cochlea. A reduction in the round window was the only prominent malformation that might be the underlying cause of the hearing impairment. However, it has been shown that ossicles malformations, along with a decrease or complete absence of the round window are not the causative anomalies of hearing loss in other *Chd7* mutant mice examined using compound action potential (CAP) (17).

Like other CHD proteins, CHD7 is predicted to have a role in histone modifications, repressing or activating downstream genes in complexes with various other proteins and transcription factors. A comprehensive expression analysis, performed by Bosman et al., presented a profile indicative of an important developmental component in all the tissues affected in CHARGE syndrome (10). The full spectrum of anomalies is therefore the result of many altered gene expression patterns and not simply the absence of a single protein. Together with two CHD family members, CHD8 and CHD9, CHD7 is considered an orthologue of the *Drosophila* Kismet, which is also a chromatin remodelling factor, known to promote transcription by mediating RNA polymerase II elongation (22). Despite the role of Kismet as an activator, and the above mentioned homology, CHD9 interacts with nuclear receptors as an activator, while CHD8 is a repressor, taking part in heterochromatin formation (23). This dichotomy raises the question whether the mechanism underlying CHARGE phenotype is a result of up-regulation or down-regulation of target genes.

A recently published chromatin immunoprecipitation on tiled microarrays suggested a clear role for CHD7 as an activator, which can directly bind H3-K4 and is mostly present at H3-K4 methylated sites, representing active DNA regions. CHD7 was mostly detected in distal sites, more than 2 kb upstream of the following promoter, in areas designated as enhancer elements. Its enhancer activity was proven using a luciferase assay and expression analysis also showed an increase in expression levels of genes present in the 10 kb surrounding CHD7 binding sites (24). As a dominant activator, lack of CHD7 would result in down-regulation of various genes that are necessary for normal development.

Nevertheless, few CHD7 binding sites have been shown to be associated with H3-K9 representing

silent DNA regions (24). It was previously reported that CHD7 is included in a protein complex, responsible for repression of the nuclear receptor PPAR-γ at target genes promoter regions. This inhibitory effect is regulated by Wnt5a as part of the non-canonical wnt signalling pathway (25). Wnt signalling is an important pathway in the development of many cell types and organs. Specifically in the inner ear, non-canonical Wnt5a is part of the planar cell polarity (PCP) mechanism, crucial for normal function of the hair cells (26). As mentioned above, no gross morphology abnormalities were identified in *Vlk* mice. However, upon close inspection of the organ of Corti, it appears that more stereociliary bundles are pointed in a different direction from normal. This phenomenon was especially apparent in the apex. Nonetheless, such hair cells were also seen to a lesser extent in the cochlea of wild-type littermates and the apex is considered less organized than more basal regions. Thus, we cannot address this as a causative phenotype. Further analysis of more sensory epithelia using PCP markers, both in the cochlea and the vestibule, might shed light on a possible genotype-phenotype correlation and the underlying mechanism of inner ear abnormalities in CHARGE patients.

In the vestibular end-organs, CHD7 pattern of expression at E12.5–E13.5 coincides with the observed phenotype of truncated canals, smaller cristae and lack of innervations to the posterior crista. The resemblance between CHD7 and Kismet implies a role for CHD7 in patterning (22). At E12.5 CHD7 is expressed in the canal pouches of the developing vestibule. According to Bosman et al. (10), the canal abnormality arises at this stage during the fusion process, so that by E13.5 the lateral canal truncation is apparent. In addition, CHD7 is also highly expressed in the vestibulo-cochlear ganglia, which might result in the lack of posterior crista innervations. This finding emphasizes the resemblance between *Vlk* and the *Chd7*-deficient mutant created by gene target mutagenesis, increasing the probability that the *Vlk* allele is a null allele, despite the occurrence of the mutation at a relatively distal portion of the protein, downstream to the important *Chd7* functional domains.

CHD7 is an important developmental gene, expressed in many tissues and cell types. As a chromatin-remodelling protein, it is incorporated upstream of various processes and pathways and together with other proteins controls the fate of many cell types. It is possible that altering mechanisms of positive and negative regulation occur not only in different organs affected in CHARGE, but even within organs, such as the cochlear and vestibular systems of the inner ear. Under normal conditions, CHD7 takes part in a variety of pathways – as an activator or as a repressor, influencing different genes. These two aspects frequently join in a common course to create an organ and, in their absence, it is difficult to determine one from the other. Thus, CHD7 haploinsufficiency is a vast combination of wrongful up-regulation and down-regulation of downstream genes in a complex pathway. The Volchok ENU-generated mutant provides one piece of this complex puzzle with insights into vestibular dysfunction on a molecular level.

Acknowledgments

This work was supported by the European Commission FP6 Integrated Projects Eumodic 037188 and EuroHear LSHG-CT-20054–512063.

Declaration of interest: The authors report no conflicts of interest. The authors alone are responsible for the content and writing of the paper.

References

1. Highstein SM. Anatomy and Physiology of the Central and Peripheral Vestibular System: Overview. In: Fay RR, Popper AN, editors. The Vestibular System. New York: Springer-Verlag; 2004. p. 1–10.
2. Bear MF, Connors BW, Paradiso MA. The Auditory and Vestibular Systems. In: Lupash E, Connolly E, Dilernia B, Williams PC, editors. Neuroscience: Exploring the Brain. Baltimore: Lippincott Williams & Wilkins; 2006. p. 343–86.
3. Petit C, Levilliers J, Hardelin JP. Molecular genetics of hearing loss. Annu Rev Genet. 2001;35:589–646.
4. Dror AA, Avraham KB. Hearing loss: mechanisms revealed by genetics and cell biology. Annu Rev Genet. 2009;43: 411–37.
5. Hrabe de Angelis MH, Flaswinkel H, Fuchs H, Rathkolb B, Soewarto D, Marschall S, et al. Genome-wide, large-scale production of mutant mice by ENU mutagenesis. Nat Genet. 2000;25:444–7.
6. Wall C 3rd, Merfeld DM, Rauch SD, Black FO. Vestibular prostheses: the engineering and biomedical issues. J Vestib Res. 2002;12:95–113.
7. Staecker H, Praetorius M, Baker K, Brough DE. Vestibular hair cell regeneration and restoration of balance function induced by math1 gene transfer. Otol Neurotol. 2007;28: 223–31.
8. Gananca CF, Caovilla HH, Gazzola JM, Gananca MM, Gananca FF. Epley's manoeuvre in benign paroxysmal positional vertigo associated with Ménière's disease. Rev Bras Otorrinolaringol (Engl Ed). 2007;73:506–12.
9. Vissers LE, van Ravenswaaij CM, Admiraal R, Hurst JA, de Vries BB, Janssen IM, et al. Mutations in a new member of the chromodomain gene family cause CHARGE syndrome. Nat Genet. 2004;36:955–7.
10. Bosman EA, Penn AC, Ambrose JC, Kettleborough R, Stemple DL, Steel KP. Multiple mutations in mouse Chd7 provide models for CHARGE syndrome. Hum Mol Genet. 2005;14:3463–76.
11. Abadie V, Wiener-Vacher S, Morisseau-Durand MP, Poree C, Amiel J, Amanou L, et al. Vestibular anomalies in CHARGE

syndrome: investigations on and consequences for postural development. Eur J Pediatr. 2000;159:569–74.
12. Delahaye A, Sznajer Y, Lyonnet S, Elmaleh-Berges M, Delpierre I, Audollent S, et al. Familial CHARGE syndrome because of CHD7 mutation: clinical intra- and inter-familial variability. Clin Genet. 2007;72:112–21.
13. Adams ME, Hurd EA, Beyer LA, Swiderski DL, Raphael Y, Martin DM. Defects in vestibular sensory epithelia and innervation in mice with loss of Chd7 function: implications for human CHARGE syndrome. J Comp Neurol. 2007;504:519–32.
14. Green EC, Gkoutos GV, Lad HV, Blake A, Weekes J, Hancock JM. EMPReSS: European mouse phenotyping resource for standardized screens. Bioinformatics. 2005;21:2930–1.
15. Self T, Sobe T, Copeland NG, Jenkins NA, Avraham KB, Steel KP. Role of myosin VI in the differentiation of cochlear hair cells. Dev Biol. 1999;214:331–41.
16. Bissonnette JP, Fekete DM. Standard atlas of the gross anatomy of the developing inner ear of the chicken. J Comp Neurol. 1996;368:620–30.
17. Kiernan AE, Erven A, Voegeling S, Peters J, Nolan P, Hunter J, et al. ENU mutagenesis reveals a highly mutable locus on mouse chromosome 4 that affects ear morphogenesis. Mamm Genome. 2002;13:142–8.
18. Alavizadeh A, Kiernan AE, Nolan P, Lo C, Steel KP, Bucan M. The Wheels mutation in the mouse causes vascular, hindbrain, and inner ear defects. Dev Biol. 2001;234:244–60.
19. Avni R, Elkan T, Dror AA, Shefer S, Eilam D, Avraham KB, et al. Mice with vestibular deficiency display hyperactivity, disorientation, and signs of anxiety. Behav Brain Res. 2009;202:210–7.
20. Smith PF, Darlington CL, Zheng Y. Move it or lose it: is stimulation of the vestibular system necessary for normal spatial memory? Hippocampus. 2010;20:36–43.
21. Kandler K, Clause A, Noh J. Tonotopic reorganization of developing auditory brainstem circuits. Nat Neurosci. 2009;12:711–7.
22. Srinivasan S, Dorighi KM, Tamkun JW. Drosophila Kismet regulates histone H3 lysine 27 methylation and early elongation by RNA polymerase II. PLoS Genet. 2008;4:1000217.
23. Hall JA, Georgel PT. CHD proteins: a diverse family with strong ties. Biochem Cell Biol. 2007;85:463–76.
24. Schnetz MP, Bartels CF, Shastri K, Balasubramanian D, Zentner GE, Balaji R, et al. Genomic distribution of CHD7 on chromatin tracks H3K4 methylation patterns. Genome Res. 2009;19:590–601.
25. Takada I, Mihara M, Suzawa M, Ohtake F, Kobayashi S, Igarashi M, et al. A histone lysine methyltransferase activated by non-canonical Wnt signalling suppresses PPAR-gamma transactivation. Nat Cell Biol. 2007;9:1273–85.
26. Qian D, Jones C, Rzadzinska A, Mark S, Zhang X, Steel KP, et al. Wnt5a functions in planar cell polarity regulation in mice. Dev Biol. 2007;306:121–33.